ORIGINAL ARTICLE

WILEY Cancer Science

High expression of CD44v9 and xCT in chemoresistant hepatocellular carcinoma: Potential targets by sulfasalazine

Fumitaka Wada[1,2] | Hironori Koga[1,2] (iD) | Jun Akiba[3] | Takashi Niizeki[1] | Hideki Iwamoto[1,2] | Yu Ikezono[1,2] | Toru Nakamura[1,2] | Mitsuhiko Abe[1,2] | Atsutaka Masuda[1,2] | Takahiko Sakaue[1,2] | Toshimitsu Tanaka[1,2] | Tatsuyuki Kakuma[4] | Hirohisa Yano[3] | Takuji Torimura[1,2]

[1]Division of Gastroenterology, Department of Medicine, Kurume University School of Medicine, Kurume, Japan

[2]Liver Cancer Research Division, Research Center for Innovative Cancer Therapy, Kurume University, Kurume, Japan

[3]Department of Pathology, Kurume University School of Medicine, Kurume, Japan

[4]Biostatistics Center, Kurume University, Kurume, Japan

Correspondence: Hironori Koga, Division of Gastroenterology, Department of Medicine, Kurume University School of Medicine, 67 Asahi-machi, Kurume 830-0011, Japan (hirokoga@med.kurume-u.ac.jp).

CD44v9 is expressed in cancer stem cells (CSC) and stabilizes the glutamate-cystine transporter xCT on the cytoplasmic membrane, thereby decreasing intracellular levels of reactive oxygen species (ROS). This mechanism confers ROS resistance to CSC and CD44v9-expressing cancer cells. The aims of the present study were to assess: (i) expression status of CD44v9 and xCT in hepatocellular carcinoma (HCC) tissues, including those derived from patients treated with hepatic arterial infusion chemoembolization (HAIC) therapy with cisplatin (CDDP); and (ii) whether combination of CDDP with sulfasalazine (SASP), an inhibitor of xCT, was more effective on tumor cells than CDDP alone by inducing ROS-mediated apoptosis. Twenty non-pre-treated HCC tissues and 7 HCC tissues administered HAIC therapy with CDDP before surgical resection were subjected to immunohistochemistry analysis of CD44v9 and xCT expression. Human HCC cell lines HAK-1A and HAK-1B were used in this study; the latter was also used for xenograft experiments in nude mice to assess in vivo efficacy of combination treatment. CD44v9 positivity was significantly higher in HAIC-treated tissues (5/7) than in non-pretreated tissues (2/30), suggesting the involvement of CD44v9 in the resistance to HAIC. xCT was significantly expressed in poorly differentiated HCC tissues. Combination treatment effectively killed the CD44v9-harboring HAK-1B cells through ROS-mediated apoptosis and significantly decreased xenografted tumor growth. In conclusion, the xCT inhibitor SASP augmented ROS-mediated apoptosis in CDDP-treated HCC cells, in which the CD44v9-xCT system functioned. As CD44v9 is typically expressed in HAIC-resistant HCC cells, combination treatment with SASP with CDDP may overcome such drug resistance.

KEYWORDS

anticancer drug resistance, cancer stem cell, combinational therapy, oxidative stress, sphere formation

1 | INTRODUCTION

Hepatocellular carcinoma (HCC) is the sixth most frequent cancer worldwide with over 740 000 new cases per year and the third leading cause of cancer-related deaths, with a growing incidence in recent years.[1] Despite early diagnosis of small HCC, it remains difficult to treat advanced-stage disease because of its high potential of intra- and extrahepatic multiple metastases and refractoriness to chemotherapeutic treatments, including transcatheter arterial chemoembolization (TACE),[2] hepatic arterial infusion chemoembolization (HAIC),[3] and the molecular-targeted drug sorafenib.[4] To overcome limitations in therapeutic efficacy, novel drugs targeting tumor refractoriness are needed. Refractoriness to chemotherapeutic treatments is attributable to the unique biological features of cancer stem cells (CSC) or CSC-like cells.[5] These cells consist of a small population of cancer cells that are capable of self-renewal and tumor initiation.[6] Therefore, targeting CSC or CSC-like cells is a key strategy for improving the outcomes of cancer patients. In HCC, markers for CSC are thought to include CD13,[7] CD44,[8] CD90,[9] CD133,[10] EpCAM,[11] and aldehyde dehydrogenase,[12] but no agents specifically targeting CSC have been developed.

CD44 is a transmembrane protein and functions as a cellular adhesion molecule for hyaluronic acid, a major component of the extracellular matrix. This molecule plays important roles in various physiological and pathological processes, including tumor cell proliferation, invasion, and metastasis.[13] It has also been identified as a cell surface marker for CSC of solid tumors. Of the several splice variant isoforms of CD44, variant 9 (v9) was recently found in CSC,[14] where it binds to xCT, a subunit of a cystine-glutamate antiporter known as system xc(−). Such binding stabilizes expression of this transporter system at the cell surface and thereby promotes intracellular synthesis of the antioxidant glutathione (GSH) from incorporated cysteine.[15] Thus, expression of CD44v9 in tumor cells confers resistance to oxidative stress and promotes tumor growth and resistance to treatments.

Salazosulfapyridine (SASP), a well-known agent used to treat ulcerative colitis and rheumatoid arthritis, is a specific inhibitor of xCT-mediated cystine transport and suppresses the proliferation of CD44v-positive cancer cells.[16] In animal models, ablation of this system suppressed cancer growth and in patients with advanced gastric cancer, SASP reduced the CD44v-positive cancer cell population and decreased intratumoral GSH levels.[17] These findings suggest that SASP is a safe and potential therapeutic agent targeting CD44v-expressing stem cell-like cancer cells in the clinical setting.

In HCC, the effect of CD44 and its isoforms on tumor aggressiveness and prognosis of patients is unclear. Recently, high expression levels of CD44v9 were observed as a potential biomarker of poor prognosis in patients with HCC.[18] However, the expression status of both CD44v9 and xCT in resistant HCC cells to chemotherapeutic treatment has not been investigated. In the present study, we observed higher expression of the CD44v9/xCT system in surviving HCC cells after HAIC therapy than in those unexposed to chemotherapeutic agents prior to surgical resection. These findings provide mechanistic insights into how SASP targets the system and induces reactive oxygen species (ROS)-mediated apoptosis in HCC cells.

2 | MATERIALS AND METHODS

2.1 | Patients and tumor tissues

Thirty-seven patients (28 males and 9 females) with HCC were enrolled in this study (Table 1). They underwent curative hepatectomy between 2000 and 2015 at Kurume University Hospital. Mean age of the patients was 71 years (range, 53-84 years). Three patients were positive for hepatitis B surface antigen, and 26 were positive for anti-hepatitis C virus antibody. HCC tissues consisted of 30 primarily resected tissues and 7 pretreated by HAIC therapy with a combination of lipiodol-suspended cisplatin (CDDP) and continuous infusion of 5-fluorouracil (5-FU).[3] Pretreated patients underwent curative resection of primary HCC after diagnosis of disappearance of pulmonary metastatic foci (patient no. 31), elimination of portal vein thrombosis (nos 32 and 37), and remarkable shrinkage of the primary tumor (nos 33, 34, 35, 36, 37) after HAIC therapy. Average maximum diameter of HCC was 37 mm (range, 10-110 mm) (Table 1). Informed consent to participate in the study was obtained from all patients in accordance with the principles stated in the Declaration of Helsinki and guidelines of the Ethical Committee of Kurume University (study registration no. 15120; Committee Chair, Kensei Nagata).

2.2 | Chemicals

Dimethyl sulfoxide, SASP, and the antioxidant N-acetylcysteine (NAC) were purchased from Sigma-Aldrich (St Louis, MO, USA). CDDP was from Wako Pure Chemical Industries, Ltd (Osaka, Japan).

2.3 | Cell lines and culture conditions

Human liver cancer cell lines Huh7 and HepG2 were obtained from the ATCC (Manassas, VA, USA). HAK-1A and HAK-1B were established and maintained in our institute.[19] HAK-1A and HAK-1B cells are well-differentiated and poorly differentiated HCC cells, respectively, and the latter are presumed to be derived from HAK-1A through clonal dedifferentiation based on p53 mutation analysis.[19] HAK-1B cells are well characterized and commonly used for subcutaneous transplantation into nude mice.[20] Human colorectal cancer cell line HCT116 was purchased from RIKEN BioResource Center (Tsukuba, Japan). All cell lines were grown in DMEM (Wako) supplemented with 10% heat-inactivated (56°C, 30 min) FBS (Biowest, Nuaillé, France), 100 U/mL penicillin, and 100 mg/mL streptomycin (Nacalai Tesque, Kyoto, Japan) in a humidified atmosphere containing 5% CO_2 at 37°C.

TABLE 1 Patient characteristics and histological features of HCC

Patient no.	Age	Gender	LC	Serum HBsAg	Anti-HCV Ab	Size of tumor (mm)	Histological pattern	Histological grading	Prior treatment
1	71	M	–	–	+	20 × 20	PS	WD	–
2	69	F	–	–	+	29 × 23	TR	WD	–
3	62	M	–	–	+	14 × 13	TR	WD	–
4	72	F	+	–	+	19 × 15	TR	WD	–
5	76	M	+	–	+	15 × 14	TR >PS	WD	–
6	69	M	–	–	+	22 × 20	TR >PS	WD	–
7	73	M	+	–	–	28 × 24	TR	WD	–
8	74	M	+	+	–	12 × 10	TR >PS	WD	–
9	69	M	+	–	+	25 × 20	TR >PS	WD	–
10	75	M	–	–	+	27 × 25	TR >PS	WD	–
11	73	M	+	–	+	28 × 25	TR	MD	–
12	71	M	+	–	+	30 × 28	TR	MD	–
13	81	M	–	–	–	38 × 38	TR >PS	MD	–
14	64	M	–	–	+	33 × 31	TR	MD	–
15	75	M	+	–	+	44 × 43	TR	MD	–
16	70	M	–	–	+	30 × 26	TR >PS	MD	–
17	56	M	+	–	+	43 × 25	TR	MD	–
18	58	F	+	+	–	28 × 22	TR	MD	–
19	75	F	–	–	+	21 × 20	TR >PS	MD	–
20	81	F	–	–	+	33 × 31	TR	MD	–
21	77	M	+	–	+	45 × 40	COM	MD	–
22	75	M	+	–	+	35 × 30	COM >TR	PD	–
23	63	M	–	–	+	70 × 60	TR	PD	–
24	77	M	–	–	–	15 × 14	COM >TR	PD	–
25	54	M	–	+	–	60 × 44	COM	PD	–
26	53	M	+	–	+	42 × 35	COM >TR	PD	–
27	78	F	–	–	+	73 × 60	TR >PS	PD	–
28	74	M	–	–	+	63 × 52	COM >TR	PD	–
29	58	M	–	–	–	43 × 30	COM	PD	–
30	80	F	+	–	–	30 × 17	COM >TR	PD	–
31	72	F	–	–	–	110 × 70	TR	MD + PD	HAIC
32	77	M	–	–	+	11 × 9	TR	MD + PD	HAIC
33	84	M	+	–	–	55 × 50	TR >PS	MD	HAIC
34	75	M	–	–	+	45 × 40	TR	MD	HAIC
35	62	M	–	–	+	50 × 45	TR >PS	MD	HAIC
36	84	M	–	–	–	61 × 49	TR >PS	MD	HAIC
37	73	F	–	–	+	10 × 7	TR	MD	HAIC

COM, compact; HAIC, hepatic arterial infusion chemoembolization; HBsAg, hepatitis B surface antigen; HCC, hepatocellular carcinoma; HCV, hepatitis C virus; LC, liver cirrhosis; MD, moderately differentiated; PD, poorly differentiated; PS, pseudoglandular; TR, trabecular; WD, well differentiated; –, none.

2.4 | Cell proliferation assay

Cell proliferation was evaluated by counting the viable cells in suspension prepared with Trypsin-EDTA solution (Nacalai Tesque) using a CDA-500 automated cell counter (Sysmex, Kobe, Japan) at days 0, 2, 4, and 6 after the treatments with DMSO alone, CDDP alone, SASP alone, and a combination of CDDP with SASP. To determine cytotoxicity-promoting concentration of SASP under combination treatment with CDDP, HAK-1B cells (1×10^4 cells/ well in a 6-well plate) were treated with different concentrations of CDDP (0, 10, 20, 40, 80, and 100 µM) with or without SASP at concentrations of 0, 50, and 100 µM for 6 days. Subsequently, the viable cell number was counted using the CDA-500 cell counter.

2.5 | Measurement of intracellular ROS

A total of 1×10^4 HAK-1B cells/well were seeded in a white 96-well plate (Thermo Fisher Scientific, Waltham, MA, USA) 2 days before the analysis. ROS levels were measured using the ROS-Glo H_2O_2 Assay kit (Promega Corporation, Madison, WI, USA) according to the manufacturer's instructions. Briefly, the cells were incubated with ROS-Glo Detection Solution for 20 minutes before treatment with different concentrations of SASP at (0, 50, and 100 μM) and CDDP (0 and 20 μM) with or without 1 mM NAC for 6 hours. Cell-derived ROS in the plates were analyzed using the GLOMAX-Multi+ Luminescence System (Promega). ROS levels were determined as values relative to untreated control. Each assay was carried out in triplicate.

2.6 | Glutathione assay

Intracellular levels of GSH were measured using the GSH-Glo Glutathione Assay kit (Promega) according to the manufacturer's instructions. First, 1×10^4 HAK-1B cells/well were cultured in a white 96-well plate overnight and treated with 20 μM CDDP, with DMSO vehicle as a control, with or without SASP at concentrations of 0, 50, and 100 μM for 3 hours. The cells were washed with water and GSH-Glo reagent was added to the plate. After incubation, luciferin detection reagent was added and luminescence was measured using the GLOMAX-Multi+ Luminescence System (Promega). All measured GSH concentrations were normalized by the cell number counted at the time of measurement. Total GSH concentration was determined from a standard curve prepared using known GSH concentrations. All experiments were conducted in triplicate.

2.7 | Sphere formation assay

HAK-1B-derived single-cell suspensions $(1.2 \times 10^4$ cells/well) were added to Ultra Low Attachment 6-well plates (Corning, Inc., Corning, NY, USA). The cells were treated with SASP alone (0, 50, and 100 μM) and in combination with 50 μM CDDP. After 14 days, the number of cell aggregates/spheres per well was quantified and photographed under a KEYENCE BZ-X700 Fluorescence Microscope (KEYENCE, Osaka, Japan). The area of the cell aggregates was measured using MetaMorph 6.0 software (Molecular Devices, Sunnyvale, CA, USA).

2.8 | Western blotting

Cells were lysed with RIPA buffer (Pierce, Rockford, IL, USA) containing Protease Inhibitor Cocktail (Nacalai Tesque) and Halt Phosphatase Inhibitor Cocktail (Pierce). Protein concentrations were measured using the BCA Protein Assay Kit (Pierce). Samples containing 25 μg protein were separated on 8% or 10% SDS-PAGE and then transferred to equilibrated PVDF membranes (Bio-Rad, Hercules, CA, USA). After blocking with 5% non-fat milk, the membranes were incubated with diluted primary antibodies overnight at 4°C. The primary antibodies for CD44 standard (CD44s) (rabbit

monoclonal), xCT (rabbit monoclonal), cleaved poly (ADP-ribose) polymerase (PARP) (rabbit polyclonal), PARP (rabbit polyclonal), cleaved caspase-3 (rabbit polyclonal), and caspase-3 (rabbit polyclonal) were purchased from Cell Signaling Technology (Danvers, MA, USA), and the antibody for CD44 variant 9 (CD44v9) (rat monoclonal) was from Cosmo Bio (Tokyo, Japan). Bound antibodies were detected with HRP-labeled secondary antibodies using ImmunoStar LD (Wako). Positive signals from the target proteins were visualized using an image analyzer (LAS-4000; Fujifilm, Tokyo, Japan).

2.9 | Immunohistochemistry and staining score

Immunohistochemistry for CD44v9 (rabbit monoclonal; Cosmo Bio) and xCT (rabbit monoclonal; Cell Signaling Technology) was carried out using the VECTASTAIN ABC kit (Vector Laboratories, Burlingame, CA, USA). Paraffin-embedded tissue sections were deparaffinized and heated in 10 mM sodium citrate buffer (pH 6.0) at 121°C for 5 minutes for antigen retrieval. Sections were preblocked with normal horse serum from the kit and incubated with the primary antibodies at 4°C overnight. According to the manufacturer's protocol, positive signals were visualized by 0.1% 3,3′-diaminobenzidine-tetrahydrochloride. Cell nuclei were counterstained with hematoxylin. Samples incubated with rat or rabbit IgG were used as negative controls. Intensity of staining was scored on a scale of 0-3 as follows: 0, negative staining; 1, mildly positive staining; 2, moderately positive staining; and 3, strongly positive staining. The signal positive area was scored on a scale of 0-3 as follows: 0, negative staining; 1, positive staining in 1%-10% of cells; 2, positive staining in 11%-60% of cells; and 3, positive staining in 61%-100% of cells. The scores were summed for each specimen. A total score of ≥1 was considered as positive expression.

2.10 | Xenograft model

HAK-1B cells $(5 \times 10^6$ per mouse) were s.c. injected into the backs of 5-week-old male BALB/c athymic nude mice (n = 15) (Clea Japan, Tokyo, Japan). Tumor size was measured weekly in 2 orthogonal directions using calipers, and tumor volume (mm^3) was estimated using the equation length × (width)^2 × 0.5. We determined the correct dosages of CDDP and SASP according to the previous report to maximize their antitumor effects and minimize adverse effects.[16] CDDP (1 mg/kg) or DMSO was injected to mice i.p., and SASP suspension (250 mg/kg) was given each day orally by gavage to avoid i.p.-related panperitonitis. In this study, the reported dosage of CDDP (2 mg/kg per injection twice per week for 4 weeks)[16] caused severe renal tubular damage, and therefore we decreased the dosage to 1 mg/kg per injection 3 times per week for 5 weeks. SASP was given orally because i.p. dosage of 250 mg/kg per injection twice per week for 4 weeks[16] caused fatal peritonitis. Tumor-bearing mice (n = 15) were randomly assigned to 3 groups of 5 mice as follows: group 1, control i.p. given DMSO 3 times per week (total 15 mg/kg); group 2, i.p. given CDDP 3 times per week (total 15 mg/kg); and group 3, i.p. given CDDP 3 times per week (total 15 mg/kg) and
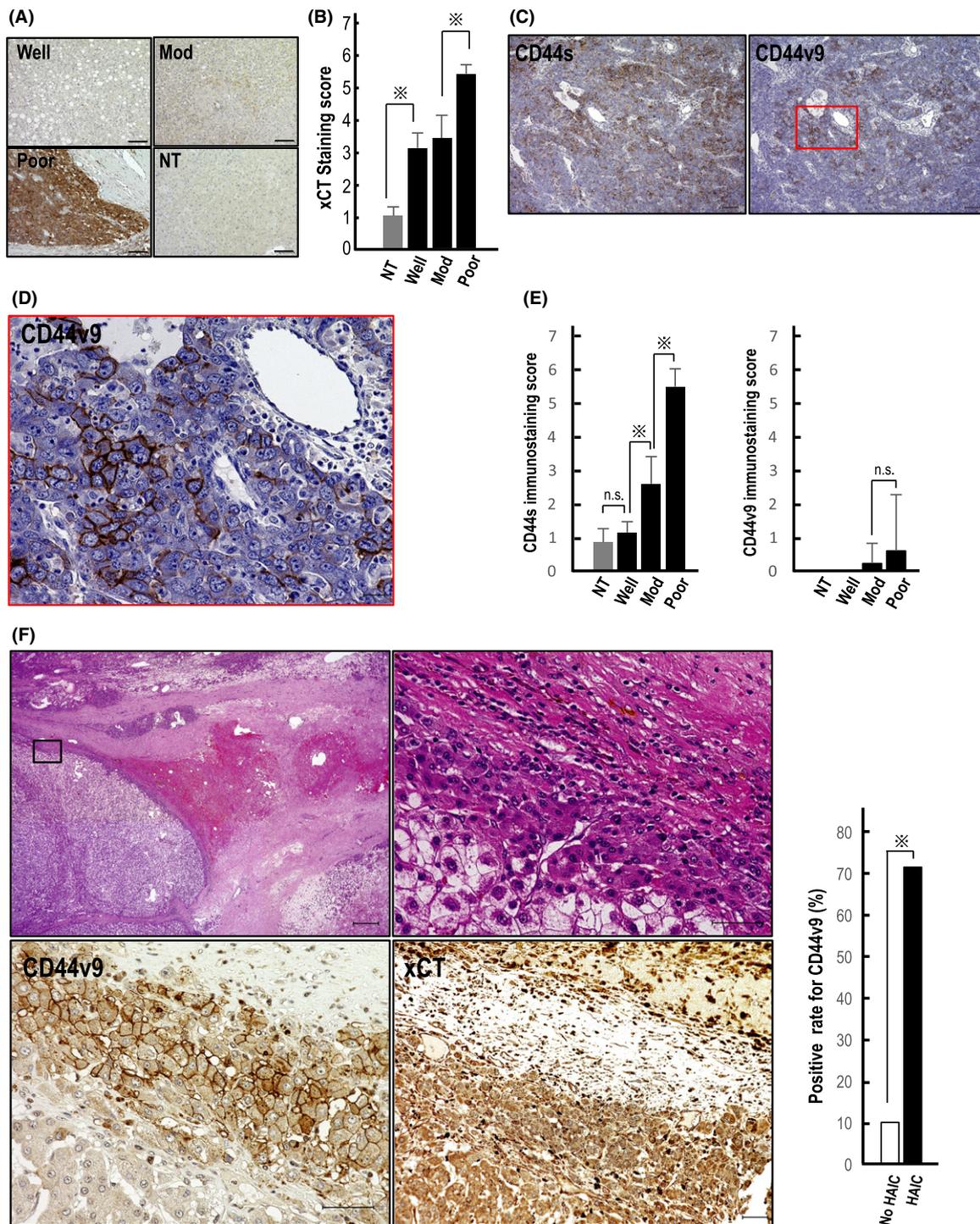
FIGURE 1 Expression of xCT, CD44s, and CD44v9 in human hepatocellular carcinoma (HCC) tissues. A, xCT is highly expressed in poorly differentiated HCC tissue (Poor), followed by moderately differentiated (Mod) and well-differentiated tissues (Well). NT, non-tumorous tissue. Scale bars, 100 μm. B, Immunostaining score shows significantly highest expression of xCT in Poor. ※$P < 0.01$; C, Limited number of CD44v9-positive HCC cells was observed among several CD44s-positive cells in Poor. Scale bars, 100 μm. D, CD44v9 was clearly localized to the cytoplasmic membrane of HCC cells (magnified view of the squared area in C)). Scale bar, 20 μm. E, Immunostaining scores for 30 HCC tissues studied. CD44v9 was positive in only 2 HCC: untreated with neoadjuvant chemotherapy and presurgical radiation therapy ※$P < 0.01$; n.s., not significant. F, (left upper panel) H&E staining of HCC tissue after hepatic arterial infusion chemoembolization (HAIC) treatment shows a viable tumor cell cluster surrounded by necrotic tissue area. Scale bar, 500 μm. (right upper panel) Magnified view of the squared area in the left upper panel. Scale bar, 50 μm. (left lower panel) CD44v9-positive HCC cells were observed at the periphery of the tumor pretreated with neoadjuvant HAIC therapy. Scale bar, 50 μm. (right lower panel) xCT was strongly positive in the same tumor area in the serial section. Scale bar, 50 μm. Graph shows that CD44v9 positivity was significantly higher in HAIC-pretreated HCC tissues (71.4%) than in those without presurgical treatments (10.0%). ※$P < 0.01$

SASP suspension (250 mg/kg) orally every day. Treatments were started when the estimated tumor volume reached approximately 30 mm^3. The mice were killed at week 5 after the start of treatment and tumors were resected. Tumor tissues were subjected to H&E staining and immunohistochemistry. All animal experiments were conducted in accordance with the NIH Guidelines for the Care and Use of Laboratory Animals and were approved by the Animal Care and Use Committee of the University of Kurume.

2.11 | Statistical analysis

All data were expressed as mean ± SD. Kruskal-Wallis rank test was carried out to examine the overall significance. If the test result was significant or showed a trend, Conover-Iman pairwise test, which controls the family-wise error rate to 0.05, was carried out. A mixed-effect model was fitted for xenografted tumor volume data. Bonferroni adjustment was used to control multiplicity. Non-parametric analyses were carried out using STATA/MP 15.1 (StataCorp LLC, College Station, TX, USA) and SAS9.4 (SAS Institute Inc., Cary, NC, USA) was used to fit the mixed models. $P < 0.05$ was considered statistically significant.

3 | RESULTS

3.1 | Expression levels of xCT, CD44v9, and CD44s in human HCC tissues

xCT was diffusely expressed in the cytoplasm of tumor cells in resected HCC tissues without neoadjuvant chemotherapy, and staining intensity was significantly stronger in HCC tissues than in histologically normal liver tissues (Figure 1A,B). The positive signal for xCT was highest in poorly differentiated HCC tissues. CD44s and CD44v9 expression was observed in the cytoplasmic membrane of HCC cells (Figure 1C,D), but CD44v9 was expressed in limited areas

of only 2 HCC tissues (patient nos 21 and 27) showing moderate and poor differentiation, respectively (Figure 1C,D). Immunostaining scores for 30 HCC tissues studied are shown in Figure 1E. Expression level of CD44s was highest in poorly differentiated HCC among the 3 histological grades of HCC, followed by moderately differentiated and well-differentiated HCC (Figure 1E). In contrast to the low CD44v9 positivity in resected HCC tissues without neoadjuvant chemotherapy, expression was observed more often (5/7) in HAIC-treated HCC tissues obtained by subsequent surgical resection (Figure 1F and the related graph) in 5 patients (nos 33-37). xCT expression level was also high in those tissues and showed similar levels to those in primarily resected tissues (Figure 1F).

3.2 | Expressions of CD44v9 and xCT in human HCC cell lines

Although the expression level of CD44v9 was not so high in the cells examined, the level was significantly higher in the aggressive HCC cell line HAK-1B than in the well-differentiated counterpart HAK-1A cells (Figure 2A). xCT levels were also high in HAK-1B (Figure 2A), which is consistent with its expression status in clinical samples. Because CD44v9 is a marker protein of CSC known to be condensed in cancer cell spheres/aggregates, we examined whether CD44v9 expression was increased in spheres/aggregates of HAK-1A and HAK-1B cells. Indeed, the expression was high in sphere-forming tumor cells, coupled with increased xCT expression (Figure 2B). This was also confirmed in other liver cancer cell lines, such as Huh7 and HepG2 cells (Figure 2C).

3.3 | Synergistic proliferation-inhibitory effects of CDDP plus SASP on HCC cells

Because CDDP is a key drug used in chemotherapy for HCC, we focused on its cytotoxic effect and possible augmentation under
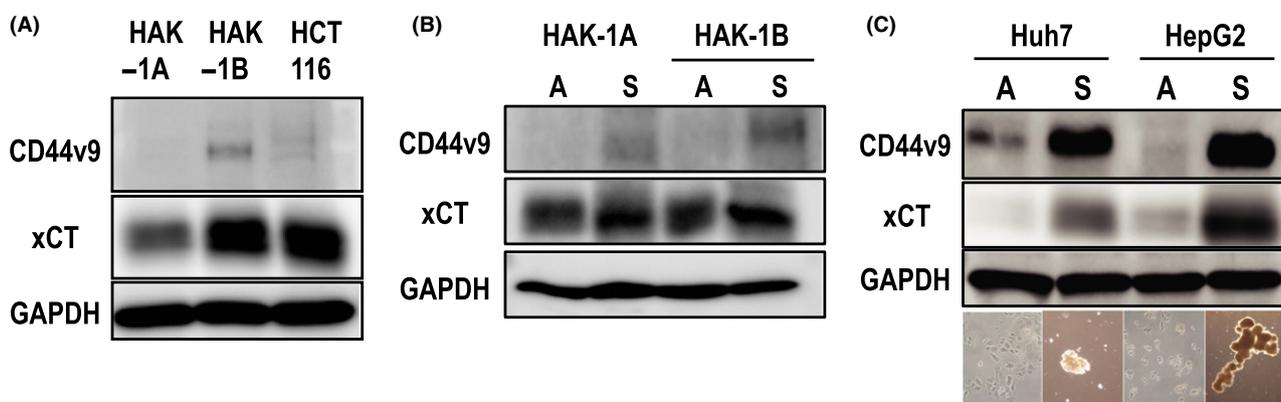

FIGURE 2 Western blotting for CD44v9 and xCT in human hepatocellular carcinoma (HCC) cell lines. A, HAK-1B strongly and weakly expresses xCT and CD44v9, respectively, compared to HAK-1A, a well-differentiated HCC cell line. The colon cancer cell line HCT-116 served as a positive control for both molecules. B, Cancer cells forming cancer spheres (S) strongly express both CD44v9 and xCT compared to those under attached conditions (A). C, Condensation of both molecules was universally observed in other liver cancer cell lines, such as Huh7 and HepG2. Phase contrast images of attached and sphere-forming cells are shown at the bottom

FIGURE 3 Inhibition of cell proliferation by cisplatin (CDDP) plus sulfasalazine (SASP) in hepatocellular carcinoma (HCC) cells. A, Synergistic inhibition of cell proliferation is significant at ≥40 μM CDDP in combination with 100 μM SASP in HAK-1B cells (※P < 0.01). B, A synergistic inhibitory effect was seen even in sphere-forming HAK-1B cells. As described in Materials and Methods, imaging analysis of the number of cell aggregates/spheres per well was conducted and the cell aggregate area (%) is shown. ※P < 0.01
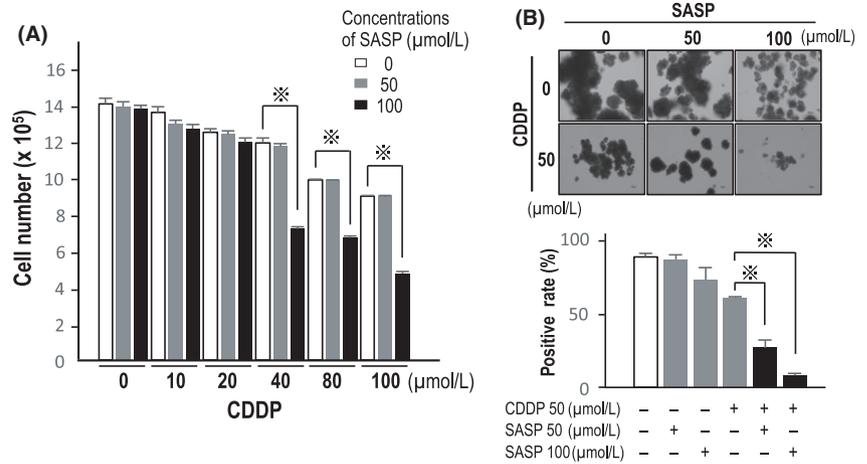
FIGURE 4 Reactive oxygen species (ROS)-dependent apoptosis enhanced by sulfasalazine (SASP). A, SASP significantly increases intracellular ROS levels in HAK-1B cells cotreated with cisplatin (CDDP) in a dose-dependent way. N-Acetylcysteine (NAC) completely inhibited ROS production. ※※P < 0.001. B, Decrease in intracellular glutathione (GSH) content was slow but significant in cells exposed to CDDP and 100 μM SASP. ※P < 0.01. C, In western blotting, the apoptosis markers cleaved (Cl) poly (ADP-ribose) polymerase (PARP) and cleaved caspase (Cas)-3 were clearly observed in cells treated with both CDDP and SASP. When these cotreated cells were exposed to NAC, apoptosis was remarkably suppressed (lane 5)
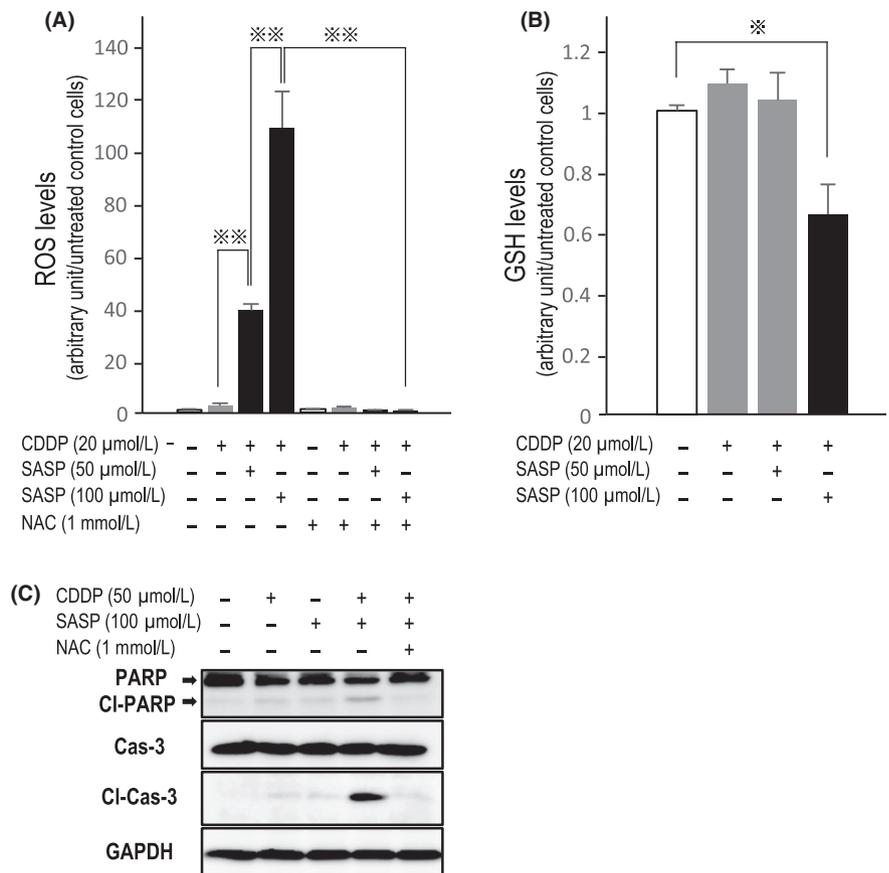
combined use with SASP on CD44v9/xCT-expressing HAK-1B cells. HAK-1A cells, in which CD44v9 expression was low or absent and xCT expression was low, were highly sensitive to CDDP alone and thus were not suitable for testing the synergistic cytotoxic effect (data not shown). As shown in Figure 3A, synergistic inhibition of cell proliferation was significant at ≥40 μM CDDP in combination with 100 μM SASP in HAK-1B cells. This synergistic inhibition was also observed in sphere-forming HAK-1B cells expressing high levels of CD44v9/xCT (Figure 3B), suggesting that the proliferation of the CSC-like cell-rich population can be decreased by combination treatment with a relatively low dosage of CDDP with SASP, which is relevant to blood concentration.[21]

3.4 | Sulfasalazine enhanced ROS-dependent apoptosis by CDDP

Because SASP was predicted to attenuate the antioxidative potential of HAK-1B cells by targeting the xCT system, we measured intracellular ROS and GSH levels in CDDP-exposed cells with or without SASP. As expected, intracellular ROS levels were robustly increased following coincubation with SASP in a dose-dependent way (Figure 4A); this increase was clearly abrogated by the antioxidant NAC (Figure 4A). A sharp but a significant decrease in GSH content was observed in cells treated with both CDDP and 100 μM of SASP (Figure 4B), indicating that the drastic increase in ROS production

occurred through GSH exhaustion (Figure 4A). Subsequently, we examined whether CDDP/SASP-treated cells were killed through ROS-dependent apoptosis by western blotting and confirmed that caspase-mediated-and ROS-dependent apoptosis was augmented by concomitant treatment with CDDP and SASP, which was clearly inhibited by NAC (Figure 4C).

3.5 | Sulfasalazine inhibited xenografted tumor growth in combination with CDDP

The size of xenografted tumors was decreased by treatments with CDDP alone and CDDP with SASP (Figure 5A). Tumor size was not significantly decreased by treatment with SASP alone at the dosage used in the present study (Figure S1). At 2 weeks after beginning treatment with CDDP and SASP, xenografted tumor growth began to be inhibited compared to that shown in mice treated with CDDP alone (Figure 5B). After 5 weeks of the combined treatment, tumor growth was significantly suppressed compared to that in mice treated with CDDP alone (Figure 5B). Consistent with the tumor growth inhibition, immunohistochemistry analysis of cleaved caspase-3 showed the highest significant positivity in the tumor tissues of mice treated with both CDDP and SASP (Figure 5C), suggesting that combination treatment induced robust apoptosis even in vivo. Additionally, combination treatment eliminated CD44v9-positive tumor cells from the xenografted tumors compared to treatment with DMSO (control) and CDDP alone (Figure 5D).

4 | DISCUSSION

The important findings of the present study are as follows: (i) CD44v9/xCT was robustly expressed in surviving HCC cells in surgically resected tissues after HAIC therapy; (ii) SASP induced ROS-mediated apoptosis in an aggressive HCC cell line expressing high levels of CD44v9/xCT and suppressed sphere formation in cancer cells in combination with CDDP; and (iii) combination treatment with SASP with CDDP had strong growth-inhibitory effects on xenografted HCC tumors in athymic mice.

The CSC marker protein CD44v9 is expressed in various types of cancer, including HCC, gastric cancer, and pancreatic cancer.[18,22,23] However, CD44v9 expression in HCC pretreated with a CDDP-containing chemotherapeutic regimen has not been analyzed in detail. Notably, we found that the frequency of CD44v9 expression was significantly increased not only in poorly differentiated

HCC tissues but also in HAIC-pretreated HCC tissues compared to in primarily resected tissues without pre-chemotherapy. This clinico-pathological finding strongly suggests that CD44v9-positive cells exist in poorly differentiated HCC cells and remain alive and proliferate as resistant cells to chemotherapeutic agents. Consistent with this finding, both CD44v9 and xCT expression levels were higher in the poorly differentiated HCC cell line HAK-1B than in the well-differentiated sister cell line HAK-1A, which was established from different layers of a single HCC nodule from the same patient.[19] Interestingly, the expression level of CD44v9 was enhanced in tumor cells under sphere formation, where stem cell-like and CSC-like cell populations may be increased.[24] These results also suggest that CD44v9 is a valid CSC marker in the cell lines used in this study.

Patients with advanced HCC showing favorable therapeutic response to TACE and/or HAIC should be identified before giving systemic treatments, such as sorafenib and regorafenib. One of the key drugs for TACE and HAIC is CDDP; therefore, we focused on whether combined use of CDDP with SASP killed HCC cells more efficiently compared to CDDP alone. Synergistic cytotoxic effects on HCC cells were seen by the combination of CDDP with SASP, which robustly increased intracellular levels of ROS and decreased GSH content, resulting in caspase-mediated apoptosis. Notably, the apoptotic process was inhibited by giving NAC, a strong antioxidant. This suggests that ROS are critically involved in apoptosis induced by CDDP and SASP. These findings indicate that SASP can kill CSC-featured HCC cells in combination with a key conventional anticancer agent and disrupt redox homeostasis in tumor cells. It is important that such effective cytotoxicity was observed at concentrations ranging within the blood concentrations of patients in the ordinary clinical setting.[25]

The strong growth-inhibitory effects of combination CDDP with SASP treatment on xenografted HCC tumors is promising as an alternative for HCC patients. The effects were based on induction of caspase-mediated apoptosis, as observed in our cell culture experiments. However, potential adverse effects may occur in clinical use. Although SASP can be safely given to patients with ulcerative colitis and rheumatoid arthritis,[26] it is not commonly used in patients with severe liver injury, including liver cirrhosis with Child-Pugh class B and C. Although it is not legally prohibited to give SASP to patients with inflammatory diseases complicated by Child-Pugh class A cirrhosis, its feasibility and safety must be carefully assessed in patients with advanced HCC in a well-designed phase I/II study. According to a recent study of the dose-escalation of SASP in patients with gastric cancer, adverse effects in the gastrointestinal tract, including appetite loss, vomiting, and diarrhea, were the main

FIGURE 5 Xenograft experiments in nude mice. A, Representative xenografted tumors (arrows) in nude mice are shown. Black arrows, control (DMSO); blue, cisplatin (CDDP)-treated; and red, CDDP/sulfasalazine (SASP)-treated. B, Size of xenografted tumors was significantly decreased from weeks 1-5 by treatment of CDDP alone, compared with that of controls (DMSO) ($P < 0.01$ at weeks 1, 2, and 3; $P < 0.05$ at weeks 4 and 5). At week 2 after beginning combinatorial treatment, tumor growth began decreasing compared to that observed in mice treated with CDDP alone. After 4 weeks of dual treatments, tumor growth was significantly suppressed compared to that in mice treated with CDDP alone (✕ ✕ $P < 0.001$). C, Consistent with the tumor growth inhibition, immunohistochemistry analysis of cleaved caspase-3 showed significantly highest positivity in tumor tissues of mice treated with both CDDP and SASP, suggesting that the drug combination also induces robust apoptosis in vivo (✕ ✕ means $P < 0.001$ or $P < 0.01$). D, CD44v9-positive tumor cells were eliminated from xenografted tumors exposed to both CDDP and SASP (left bottom). Scale bar, 50 μm. The staining score was calculated as described in Materials and Methods (✕ $P < 0.05$; ✕ ✕ $P < 0.001$)
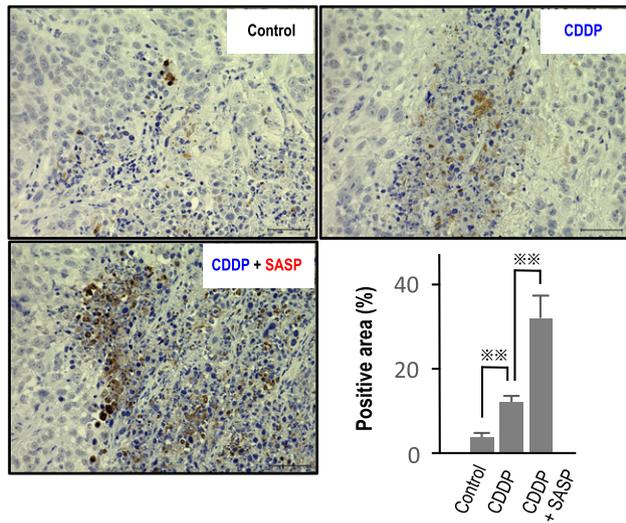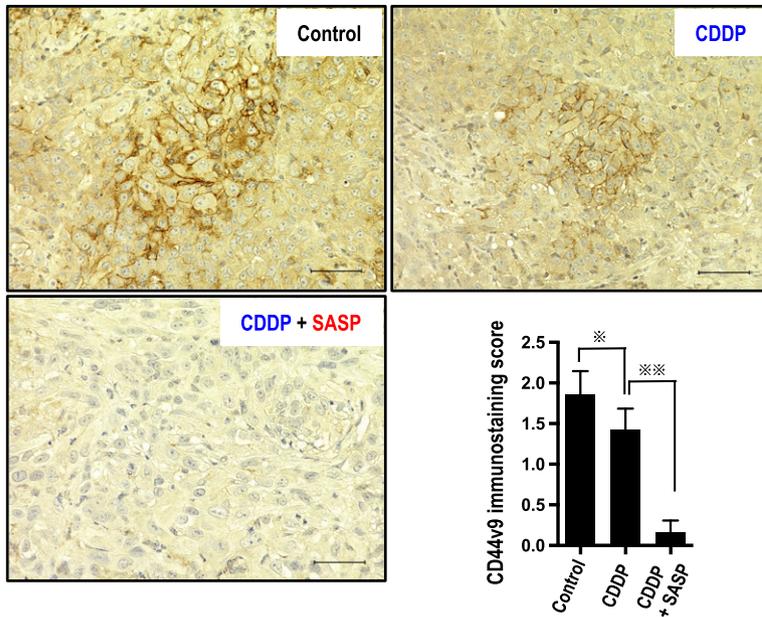
(A)
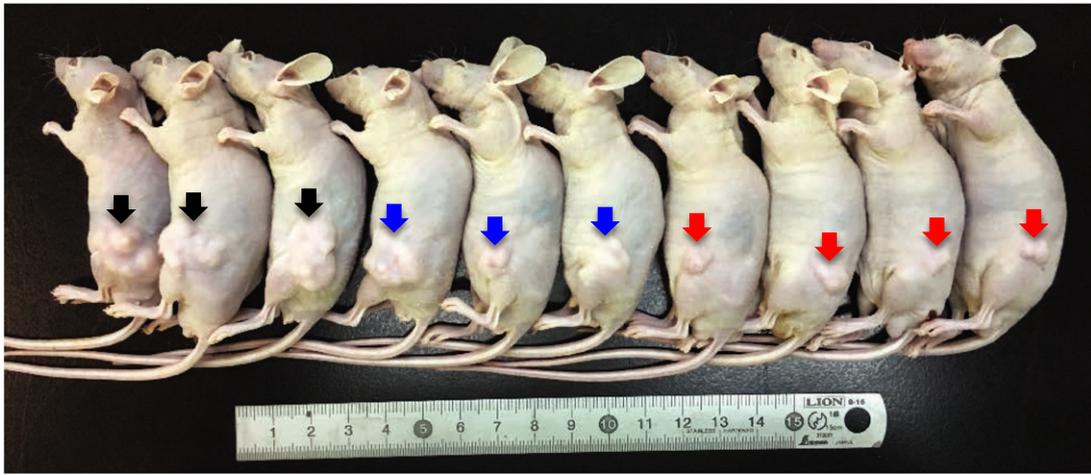
(B)
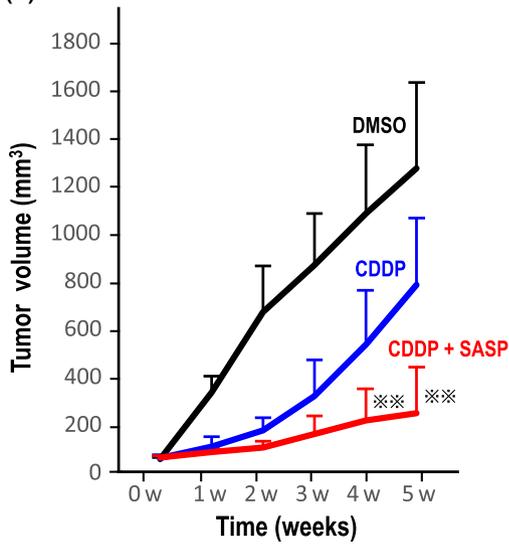
(C)

(D)

reasons for discontinuation of the study.[17] Therefore, we did not examine 5-FU, another key drug in HCC treatment, for combination dosage with SASP because 5-FU may frequently induce such gastrointestinal complications.[27] Although several molecular-targeted drugs, such as lenvatinib and immune checkpoint inhibitors,[28,29] were predicted to be effective, their efficacy limitations should be examined and novel multidisciplinary alternatives for the treatment of HCC should be developed.

CONFLICTS OF INTEREST

Authors declare no conflicts of interest for this article.

ORCID

Hironori Koga iD http://orcid.org/0000-0001-5814-9543

REFERENCES

1. White DL, Thrift AP, Kanwal F, Davila J, El-Serag HB. Incidence of hepatocellular carcinoma in all 50 United States, from 2000 through 2012. *Gastroenterology*. 2017;152:812-820.
2. Forner A, Llovet JM, Bruix J. Hepatocellular carcinoma. *Lancet*. 2012;379:1245-1255.
3. Nagamatsu H, Sumie S, Niizeki T, et al. Hepatic arterial infusion chemoembolization therapy for advanced hepatocellular carcinoma: multicenter phase II study. *Cancer Chemother Pharmacol*. 2016;77:243-250.
4. Nakano M, Tanaka M, Kuromatsu R, et al. Sorafenib for the treatment of advanced hepatocellular carcinoma with extrahepatic metastasis: a prospective multicenter cohort study. *Cancer Med*. 2015;4:1836-1843.
5. Pang RW, Poon RT. Cancer stem cell as a potential therapeutic target in hepatocellular carcinoma. *Curr Cancer Drug Targets*. 2012;12:1081-1094.
6. Bonnet D, Dick JE. Human acute myeloid leukemia is organized as a hierarchy that originates from a primitive hematopoietic cell. *Nat Med*. 1997;3:730-737.
7. Haraguchi N, Ishii H, Mimori K, et al. CD13 is a therapeutic target in human liver cancer stem cells. *J Clin Invest*. 2010;120:3326-3339.
8. Mima K, Okabe H, Ishimoto T, et al. CD44s regulates the TGF-β-mediated mesenchymal phenotype and is associated with poor prognosis in patients with hepatocellular carcinoma. *Cancer Res*. 2012;72:3414-3423.
9. Yang ZF, Ho DW, Ng MN, et al. Significance of CD90+ cancer stem cells in human liver cancer. *Cancer Cell*. 2008;13:153-166.
10. Ma S, Tang KH, Chan YP, et al. miR-130b promotes CD133(+) liver tumor-initiating cell growth and self-renewal via tumor protein 53-induced nuclear protein 1. *Cell Stem Cell*. 2010;7:694-707.
11. Yamashita T, Ji J, Budhu A, et al. EpCAM-positive hepatocellular carcinoma cells are tumor-initiating cells with stem/progenitor cell features. *Gastroenterology*. 2009;136:1012-1024.
12. Dollé L, Best J, Empsen C, et al. Successful isolation of liver progenitor cells by aldehyde dehydrogenase activity in naive mice. *Hepatology*. 2012;55:540-552.
13. Nagano O, Saya H. Mechanism and biological significance of CD44 cleavage. *Cancer Sci*. 2004;95:930-935.
14. Ishimoto T, Oshima H, Oshima M, et al. CD44+ slow-cycling tumor cell expansion is triggered by cooperative actions of Wnt and prostaglandin E2 in gastric tumorigenesis. *Cancer Sci*. 2010;101:673-678.
15. Trachootham D, Alexandre J, Huang P. Targeting cancer cells by ROS-mediated mechanisms: a radical therapeutic approach? *Nat Rev Drug Discov*. 2009;8:579-591.
16. Ishimoto T, Nagano O, Yae T, et al. CD44 variant regulates redox status in cancer cells by stabilizing the xCT subunit of system xc(-) and thereby promotes tumor growth. *Cancer Cell*. 2011;19:387-400.
17. Shitara K, Doi T, Nagano O, et al. Dose-escalation study for the targeting of CD44v(+) cancer stem cells by sulfasalazine in patients with advanced gastric cancer (EPOC1205). *Gastric Cancer*. 2017;20:341-349.
18. Kakehashi A, Ishii N, Sugihara E, et al. CD44 variant 9 is a potential biomarker of tumor initiating cells predicting survival outcome in hepatitis C virus-positive patients with resected hepatocellular carcinoma. *Cancer Sci*. 2016;107:609-618.
19. Yano H, Iemura A, Fukuda K, Mizoguchi A, Haramaki M, Kojiro M. Establishment of two distinct human hepatocellular carcinoma cell lines from a single nodule showing clonal dedifferentiation of cancer cells. *Hepatology*. 1993;18:320-327.
20. Selvendiran K, Koga H, Ueno T, et al. Luteolin promotes degradation in signal transducer and activator of transcription 3 in human hepatoma cells: an implication for the antitumor potential of flavonoids. *Cancer Res*. 2006;66:4826-4834.
21. Nagano O, Okazaki S, Saya H. Redox regulation in stem-like cancer cells by CD44 variant isoforms. *Oncogene*. 2013;32:5191-5198.
22. Hirata K, Suzuki H, Imaeda H, et al. CD44 variant 9 expression in primary early gastric cancer as a predictive marker for recurrence. *Br J Cancer*. 2013;109:379-386.
23. Li Z, Chen K, Jiang P, et al. CD44v/CD44s expression patterns are associated with the survival of pancreatic carcinoma patients. *Diagn Pathol*. 2014;9:79.
24. Chen SF, Chang YC, Nieh S, Liu CL, Yang CY, Lin YS. Nonadhesive culture system as a model of rapid sphere formation with cancer stem cell properties. *PLoS ONE*. 2012;7:e31864.
25. Gu GZ, Xia HM, Pang ZQ, Liu ZY, Jiang XG, Chen J. Determination of sulphasalazine and its main metabolite sulphapyridine and 5-aminosalicylic acid in human plasma by liquid chromatography/tandem mass spectrometry and its application to a pharmacokinetic study. *J Chromatogr B Analyt Technol Biomed Life Sci*. 2011;879:449-456.
26. Desreumaux P, Ghosh S. Review article: mode of action and delivery of 5-aminosalicylic acid - new evidence. *Aliment Pharmacol Ther*. 2006;24(Suppl 1):2-9.
27. Daniele B, Perrone F, Gallo C, et al. Oral glutamine in the prevention of fluorouracil induced intestinal toxicity: a double blind, placebo controlled, randomised trial. *Gut*. 2001;48:28-33.
28. de Rosamel L, Blanc JF. Emerging tyrosine kinase inhibitors for the treatment of hepatocellular carcinoma. *Expert Opin Emerg Drugs*. 2017;22:175-190.
29. Kudo M. Immuno-oncology in hepatocellular carcinoma: 2017 update. *Oncology*. 2017;93(Suppl 1):147-159.

SUPPORTING INFORMATION

Additional supporting information may be found online in the Supporting Information section at the end of the article.